

GENERALIZABLE SPEECH DEEPFAKE DETECTION VIA INFORMATION BOTTLENECK ENHANCED ADVERSARIAL ALIGNMENT

Pu Huang¹, Shouguang Wang^{1*}, Siya Yao¹, Mengchu Zhou^{1,2}

¹ School of Information and Electronic Engineering, Zhejiang Gongshang University, Hangzhou, China

² Department of Electrical and Computer Engineering, New Jersey Institute of Technology, Newark, USA

ABSTRACT

Neural speech synthesis techniques have enabled highly realistic speech deepfakes, posing major security risks. Speech deepfake detection is challenging due to distribution shifts across spoofing methods and variability in speakers, channels, and recording conditions. We explore learning shared discriminative features as a path to robust detection and propose Information Bottleneck enhanced Confidence-Aware Adversarial Network (IB-CAAN). Confidence-guided adversarial alignment adaptively suppresses attack-specific artifacts without erasing discriminative cues, while the information bottleneck removes nuisance variability to preserve transferable features. Experiments on ASVspoof 2019/2021, ASVspoof 5, and In-the-Wild demonstrate that IB-CAAN consistently outperforms baseline and achieves state-of-the-art performance on many benchmarks.

Index Terms— Speech deepfake detection, Information bottleneck, Adversarial alignment, Shared discriminative features

1. INTRODUCTION

Recent advances in text-to-speech and voice conversion have greatly improved the realism of synthetic speech. Such speech deepfakes are increasingly indistinguishable from natural speech, raising serious risks of fraud, disinformation, and privacy violations. These concerns highlight the urgent need for reliable detection methods [1].

Speech deepfake detection is an out-of-distribution generalization problem: detectors trained on limited spoofing methods must generalize to unseen ones at deployment [2]. This mismatch across spoofing methods induces *concept shift* (overfitting to attack-specific artifacts). In addition, *covariate shift* arises from variability in speakers, codecs, and recording conditions, further degrading performance [3].

Existing strategies such as data augmentation [4], transfer learning [5, 6], and representation optimization [7, 8] improve robustness but often remain tied to attack-specific artifacts. A promising but under-explored direction is to learn discrimina-

tive cues shared across spoofing methods. This raises a natural question: do such shared discriminative features exist? Fortunately, empirical evidence indicates that they do indeed. For example, [9] demonstrates that different neural speech synthesis methods share common artifacts that can be captured by Transformer-based networks. Similarly, [5] shows that discriminative information within the 0.1–2.4 kHz band generalizes across datasets, while high-frequency cues may not transfer well. To leverage such cues, a common strategy is domain-invariant representation learning (DIRL) [10], such as domain adversarial training [11]. Yet in speech deepfake detection, the concept of “domain” is more subtle: artifacts function both as sources of domain shift and as critical discriminative signals. Consequently, blindly enforcing alignment may suppress informative cues while preserving irrelevant variability, thereby undermining generalization.

To address this, we propose Information Bottleneck enhanced Confidence-Aware Adversarial Network (IB-CAAN). CAAN leverages classifier confidence as an auxiliary adversarial signal to adaptively suppress harmful attack-specific artifacts, while the IB encourages compression of irrelevant input factors. Together, they guide the model to preserve cross-attack discriminative cues and learn minimal sufficient representations. Our contributions are summarized as follows:

- 1) We formalize speech deepfake detection as a dual distribution shift problem and propose to address it via attack-invariant feature learning.
- 2) We propose IB-CAAN, a novel attack-invariant feature learning framework for speech deepfake detection.
- 3) Experiments on ASVspoof 2019 LA [12], ASVspoof 2021 LA and DF [13], ASVspoof 5 [14], and In-the-Wild [2] demonstrate that IB-CAAN outperforms baseline and surpasses state-of-the-art systems on many benchmarks.

2. METHODS

2.1. Problem background

In real-world speech deepfake detection tasks, the training phase typically relies on a limited dataset

$$D_{\text{tr}} = \{(x_i, y_i)\}_{i=1}^n, (x_i, y_i) \sim P_{\text{tr}}(X, Y), \quad (1)$$

* Corresponding author.

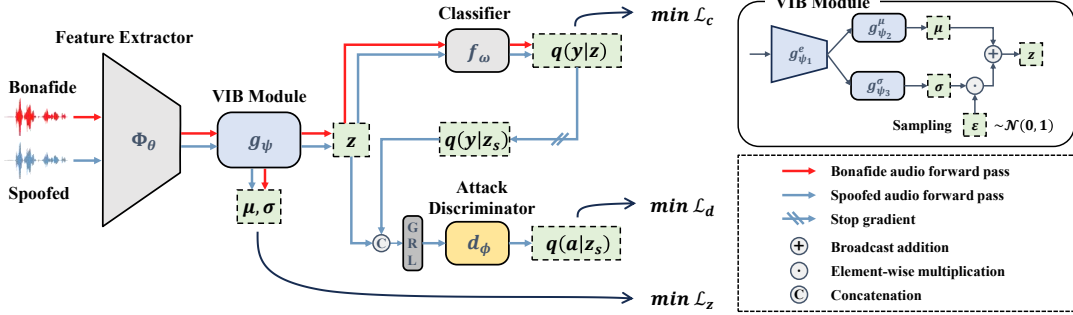


Fig. 1. The training pipeline of the proposed IB-CAAN. During inference, only Φ_θ , g_ψ , and f_ω are retained.

where X, Y denote the input and label random variables with domains \mathcal{X}, \mathcal{Y} ($\mathcal{Y} = \{0, 1\}$), and $P_{\text{tr}}(X, Y)$ is joint distribution. However, the deployed model must work in a much more complex testing environment with a different joint distribution $P_{\text{te}}(X, Y)$. This mismatch manifests as two types of distribution shift: *covariate shift* ($P_{\text{tr}}(X) \neq P_{\text{te}}(X)$, e.g., non-overlapping speakers) and *concept shift* ($P_{\text{tr}}(Y|X) \neq P_{\text{te}}(Y|X)$, e.g., unseen spoofing algorithms breaking the model’s learned decision rule).

Our goal is to learn a binary classifier $h : \mathcal{X} \rightarrow \mathcal{Y}$, that minimizes the expected risk on the test distribution:

$$R(h) = \mathbb{E}_{(x,y) \sim P_{\text{te}}(X,Y)}[\ell(h(x), y)], \quad (2)$$

where $\ell(\cdot, \cdot)$ denotes the 0–1 loss or a differentiable surrogate. However, Empirical Risk Minimization (ERM) minimizes the empirical risk on D_{tr} , i.e., $\hat{R}_{\text{tr}}(h) = \frac{1}{n} \sum_{i=1}^n \ell(h(x_i), y_i)$, which generally fails to ensure the optimality of $R(h)$.

2.2. Method overview

To address these challenges, we propose IB-CAAN, as illustrated in Fig. 1. In our design, CAAN encourages the learning of attack-invariant discriminative features, while the IB principle compresses redundant information.

2.3. Information bottleneck

To mitigate *covariate shift*, we adopt the IB principle [15]. It seeks a latent representation Z of input X that compresses irrelevant information while retaining maximal predictive information about label Y . The IB objective is formulated as:

$$\min \beta I(X; Z) - I(Z; Y), \quad (3)$$

where $I(X; Z)$ denotes the mutual information between input X and latent representation Z , and $I(Z; Y)$ denotes the mutual information between Z and output Y . β controls the trade-off between compression and prediction. Since mutual information in high-dimensional continuous spaces is intractable to compute directly, optimizing Eq. (3) is generally

infeasible. We follow the Variational Information Bottleneck (VIB) [16] and optimize its variational upper bound:

$$\beta I(X; Z) - I(Z; Y) \leq \beta \mathbb{E}_{p(x,z)} \left[\log \left(\frac{p(z|x)}{r(z)} \right) \right] - \mathbb{E}_{p(x,y,z)} [\log q(y|z)], \quad (4)$$

where $r(z)$ and $q(y|z)$ are variational approximations to the true marginal $p(z)$ and conditional $p(y|z)$, respectively. $p(z|x)$ is the conditional distribution given by an encoder. Since sampling directly from $z \sim p(z|x)$ prevents backpropagation, we apply the reparameterization trick, which rewrites the sampling process as a deterministic function of an auxiliary noise variable ϵ , i.e., $z = \mu(x) + \sigma(x) \odot \epsilon$, $\epsilon \sim \mathcal{N}(0, I)$. We assume $r(z) = \mathcal{N}(0, I)$. The encoder is parameterized by a feature extractor $\Phi_\theta(\cdot)$ and an VIB module $g_\psi(\cdot)$ which include an MLP encoder $g_{\psi_1}^e(\cdot)$, and two linear projections $g_{\psi_2}^\mu(\cdot)$ and $g_{\psi_3}^\sigma(\cdot)$. Thus, the conditional distribution is modeled as $p(z|x; g \circ \Phi) = \mathcal{N}(\mu(x), \text{diag}(\sigma(x)^2))$, with $\mu(x) = g_{\psi_2}^\mu(g_{\psi_1}^e(\Phi_\theta(x)))$, $\sigma(x) = g_{\psi_3}^\sigma(g_{\psi_1}^e(\Phi_\theta(x)))$. Finally, we optimize the following training objective:

$$\mathcal{L}_c + \beta \mathcal{L}_z = \min_{\theta, \psi, \omega} \mathbb{E}_{z \sim p(z|x; g \circ \Phi), y} [\mathcal{L}_{\text{wce}}(f_\omega(z), y)] + \beta \min_{\theta, \psi} \mathbb{E}_x [\text{KL}(p(z|x; g \circ \Phi) \| r(z))]. \quad (5)$$

Where f_ω is a binary classifier, \mathcal{L}_{wce} is weighted cross-entropy loss, and the Kullback-Leibler (KL) divergence regularizes the latent representation.

2.4. Confidence-aware adversarial Network

To alleviate *concept shift*, our goal is to enable the model to learn generalizable discriminative features shared across different spoofing algorithms. In domain generalization [10], this idea is formalized as DURL. Let z_s denote the latent representation of spoofed speech obtained from the VIB encoder, i.e., $z_s \sim p(z|x_s; g \circ \Phi)$, x_s are spoofed samples. And a main classifier $f_\omega(\cdot)$ predicts the binary label (bonafide or spoof), while a domain discriminator $d_\phi(\cdot)$ distinguishes

spooftypes. Following DANN [11], we adopt an adversarial objective between VIB module g_ψ and discriminator d_ϕ :

$$\begin{aligned} \mathcal{L}_c + \alpha \mathcal{L}_d = & \min_{\theta, \psi, \omega} \mathbb{E}_{z_s, y} \mathcal{L}_{\text{wce}}(f_\omega(z_s), y) \\ & + \alpha \min_{\phi} \max_{\theta, \psi} \mathbb{E}_{z_s, a} \mathcal{L}_{\text{ce}}(d_\phi(z_s), a), \end{aligned} \quad (6)$$

where \mathcal{L}_c is the same main classification objective as defined in Eq. (5), \mathcal{L}_{ce} is cross-entropy loss, and a is spoof type label. The min-max structure encourages the latent representation z_s to be invariant to spoof types. In practice, the maximization over (θ, ψ) is implemented via a gradient reversal layer (GRL), which keeps the forward pass unchanged but multiplies a gradient by $-\lambda$ during backward.

In the context of *concept shift*, the “domain” is induced by spoof-specific artifacts that are correlated with the main task. To analyze this, we decompose the speech feature as $X \triangleq X_0 \oplus X_1 \oplus X_2$, where X_0 denotes task-irrelevant variations, X_1 represents attack-invariant discriminative features, and X_2 captures attack-specific characteristics. However, although standard DANN aims to suppress X_2 , it may inadvertently amplify X_0 , thereby conflicting with the main task.

To address this issue, we propose the CAAN framework, in which the discriminator receives as input both the latent representations and the classifier’s confidence scores. Accordingly, the second term in Eq. (6) is reformulated as

$$\alpha \mathcal{L}_d = \alpha \min_{\phi} \max_{\theta, \psi} \mathbb{E}_{z_s, a} \mathcal{L}_{\text{ce}}(d_\phi([z_s, c(z_s)]), a), \quad (7)$$

where $c(z_s) = 1/(1 + e^{-f_\omega(z_s)})$ denotes main classifier confidences, $[\cdot]$ denotes the concatenation operation. With this design, when classifier confidence is high, \mathcal{L}_d encourages alignment that suppresses attack-specific artifacts; when confidence is low, it instead reduces spurious alignment.

2.5. Training objective

Finally, we combine the IB with CAAN by jointly optimizing:

$$\mathcal{L} = \mathcal{L}_c + \beta \mathcal{L}_z + \alpha \mathcal{L}_d, \quad (8)$$

where \mathcal{L}_c is binary classification loss, \mathcal{L}_z is IB regularization term, and \mathcal{L}_d is adversarial loss. β and α are hyperparameters that balance the loss terms.

3. EXPERIMENTS

3.1. Experimental setups

Datasets and metrics. To evaluate cross-dataset generalization, we follow the official protocols of ASVspoof 2019 [12], ASVspoof 2021 [13], and ASVspoof 5 [14]. Two groups of experiments are conducted: 1) Training on the ASVspoof 2019 LA training set (ASV19:Trn) and evaluating on eval sets of ASVspoof 2019 LA (19LA), ASVspoof 2021 LA

(21LA) and ASVspoof 2021 DF (21DF); 2) Training on the ASVspoof 5 training set (ASV5:Trn) and evaluating on ASVspoof 5 Track 1 eval set (ASV5:T1). Additionally, we perform evaluations on In-the-Wild (ITW) [2] under both training protocols. We report performance using Equal Error Rate (EER) [1].

Implementation details. All audio samples used for training and evaluation are cropped or zero-padded to approximately 4 seconds (64,600 samples). We adopt three representative backbones, which are RawBMamba [17], XLSR+Linear [5], and XLSR+MLP [18], with different training setups. Specifically, RawBMamba uses batch size 32, learning rate 1×10^{-5} , weight decay 1×10^{-4} , Adam optimizer [19] with $\beta_1 = 0.9$, $\beta_2 = 0.98$, and Noam scheduler [20], while XLSR-based backbones use batch size 12, learning rate 1×10^{-6} , weight decay 1×10^{-4} , Adam optimizer with $\beta_1 = 0.9$, $\beta_2 = 0.999$, and no scheduler. For the trade-off coefficients in training loss, we set (β, α) to $(0.001, 1)$ for RawBMamba on ASV19:Trn, $(0.001, 0.5)$ for XLSR-based backbones on ASV19:Trn, $(0.001, 0.5)$ for RawBMamba on ASV5:Trn, and $(0.01, 0.5)$ for XLSR-based backbones on ASV5:Trn. For the GRL coefficient λ , we follow [11] and adopt a schedule $\lambda_p = \frac{2}{1 + \exp(-10 \cdot p)} - 1$, which increases smoothly from 0 to 1. We consider both settings with and without data augmentation. In the augmentation setting, RawBoost [4] is applied to ASV19:Trn, and MUSAN noise [21] together with RIR [22] are applied to ASV5:Trn. Final results were obtained by averaging the top-5 checkpoints from 30 training epochs¹.

3.2. Comparison with baselines

To evaluate the effectiveness of IB-CAAN, we compare it with ERM (baseline) using three backbones, as shown in Table 1. In in-domain evaluation (19LA), IB-CAAN achieves comparable performance to ERM with RawBMamba and XLSR+Linear, while with XLSR+MLP it reduces the EER from 0.80% to 0.40%, achieving a 50% relative improvement. In out-of-domain evaluations (21LA, 21DF, ASV5:T1, and ITW), IB-CAAN consistently outperforms ERM, e.g., on ASV5:T1, IB-CAAN with XLSR+MLP reduces the EER from 8.79% to 5.98%, while on ITW it lowers the EER from 10.74% to 4.93%, showing consistent gains in cross-dataset evaluations. Notably, the gains are particularly large with XLSR-based backbones, which we attribute to the Transformer networks being more effective in capturing cross-attack discriminative cues, consistent with prior findings [9].

3.3. Comparison with state-of-the-art single systems

As shown in Table 2, without data augmentation, XLSR+MLP (IB-CAAN) significantly outperforms XLSR+AASIST under the same setting, achieving the lowest EER of 4.93% on ITW.

¹Code available at <https://github.com/763021701/IB-CAAN>

Table 1. Comparison with baselines in EER (%). The results are reported as the format of best/mean across 3 runs.

Φ_θ	f_ω	Algorithm	Train on ASV19:Trn				Train on ASV5:Trn		
			19LA	21LA	21DF	ITW	ASV5:Dev	ASV5:T1	ITW
RawBMamba	Linear	ERM	1.78 / 1.91	5.22 / 5.46	19.42 / 20.09	42.18 / 42.62	20.55 / 21.80	31.19 / 32.77	30.77 / 35.17
		IB-CAAN	1.71 / 2.24	5.01 / 5.43	19.43 / 19.90	24.60 / 27.85	17.96 / 18.52	30.59 / 31.01	21.22 / 24.46
XLSR	Linear	ERM	0.53 / 0.57	4.89 / 6.70	4.41 / 5.61	10.15 / 14.13	0.33 / 0.43	8.17 / 8.38	17.34 / 19.22
		IB-CAAN	0.37 / 0.58	4.66 / 5.06	3.28 / 3.51	5.54 / 5.99	0.18 / 0.26	6.26 / 6.31	8.51 / 13.48
XLSR	MLP	ERM	0.56 / 0.80	5.16 / 7.55	6.12 / 7.40	9.41 / 10.74	0.41 / 0.53	6.85 / 8.79	17.15 / 18.99
		IB-CAAN	0.24 / 0.40	4.00 / 4.69	3.50 / 3.75	4.61 / 4.93	0.09 / 0.12	5.96 / 5.98	8.11 / 11.62

Table 2. Results of comparison with state-of-the-art single systems on 19LA, 21LA, 21DF, and ITW in EER (%). Best results are in **bold**, and second-best results are underlined.

System	19LA	21LA	21DF	ITW
2022 XLSR+AASIST [23]	-	6.15	7.70	-
2022 XLSR+AASIST* [24]	<u>0.22</u>	0.82	2.85	10.48
2024 OCKD* [24]	0.39	<u>0.90</u>	2.27	7.68
2025 XLSR+MoE* [25]	-	2.96	2.54	9.17
2024 XLSR+SLS* [26]	-	3.88	2.09	8.87
2025 LSR+LSA* [27]	0.15	1.19	2.43	5.92
2025 XLSR+Mamba* [28]	-	0.93	1.88	6.71
2025 XLSR+Nes2Net-X* [29]	-	2.00	<u>1.78</u>	6.60
XLSR+MLP (IB-CAAN)	0.40	4.69	3.75	4.93
XLSR+MLP (IB-CAAN)*	0.31	2.21	1.64	<u>5.65</u>

* with Rawboost augmentation.

With data augmentation, the EER further decreases to 1.64% on 21DF, achieving the best performance, and our system still obtains the lowest EER on ITW with 5.65%. On 21LA, the 2.21% EER is comparable to recent advanced XLSR-based systems such as XLSR+MoE and XLSR+Nes2Net-X. For ASVspoo5 (Table 3), RawBMamba (IB-CAAN) achieves 27.77% EER under the closed condition, falling short of the best-performing submission at 23.63%, while remaining competitive compared to other strong systems. In contrast, under the open condition, XLSR+MLP (IB-CAAN) achieves 4.67% EER, establishing a new state of the art.

3.4. Ablation studies

Table 4 presents the results of ablation experiments. Removing the IB module leads to a large degradation, with the average EER rising from 3.95% to 13.92%, showing that IB plays a key role in suppressing irrelevant variations. Excluding CAAN also worsens performance, especially on ITW and ASV5:T1. Removing confidence guidance (IB-DANN) improves performance on 21LA but causes clear degradation on other datasets. The complete IB-CAAN achieves the best overall (average) performance, demonstrating that IB and CAAN are complementary for improving generalization.

Table 3. Results of comparison with state-of-the-art single systems on ASV5:T1 in EER (%). Best results are in **bold**.

Condition	System	EER
Closed	2024 T06 [14]	28.41
	2024 T19 [14]	24.59
	2024 T48 [14]	23.63
	RawBMamba (IB-CAAN)	31.01
	RawBMamba (IB-CAAN)*	27.77
Open	2022 XLSR+AASIST* [29]	6.08
	2024 T19 [14]	6.06
	2024 T17 [14]	5.99
	2025 XLSR+Nes2Net-X* [29]	5.92
	2024 T31 [14]	5.56
	XLSR+MLP (IB-CAAN)	5.98
	XLSR+MLP (IB-CAAN)*	4.67

* with Musan and RIR augmentations.

Table 4. Results of ablation experiments. Best results are in **bold**, and second-best results are underlined.

Configuration	19LA	21LA	21DF	ITW	ASV5:T1	AVG
IB-CAAN	0.40	<u>4.69</u>	3.75	4.93	5.98	3.95
w/o IB	1.07	10.33	18.29	23.40	16.50	13.92
w/o CAAN	<u>0.57</u>	5.47	<u>4.45</u>	<u>8.78</u>	9.21	5.56
IB-DANN	1.03	4.00	4.72	10.26	<u>6.64</u>	<u>5.33</u>

4. CONCLUSIONS

In this work, we introduced IB-CAAN for speech deepfake detection. IB-CAAN compresses nuisance variability and suppresses attack-specific artifacts, which facilitates learning transferable discriminative features and improves generalization. Experiments on ASVspoo5 2019/2021, ASVspoo5, and In-the-Wild datasets demonstrate that IB-CAAN consistently outperforms the ERM baseline and achieves the best performance on many benchmarks. In future work, we will further investigate attack-invariant discriminative feature learning for speech deepfake detection.

5. ACKNOWLEDGMENT

The authors used a large language model (LLM) to polish language and improve clarity. All content was reviewed, edited, and verified by the authors.

6. REFERENCES

- [1] Menglu Li, Yasaman Ahmadiadli, and Xiao-Ping Zhang, “A survey on speech deepfake detection,” *ACM Computing Surveys*, vol. 57, no. 7, pp. 1–38, 2025.
- [2] Nicolas Müller, Pavel Czepin, Franziska Diekmann, Adam Froghyar, and Konstantin Böttinger, “Does Audio Deepfake Detection Generalize?,” in *Proc. Interspeech*, 2022, pp. 2783–2787.
- [3] Ariel Cohen, Inbal Rimon, Eran Aflalo, and Haim H Permuter, “A study on data augmentation in voice anti-spoofing,” *Speech Communication*, vol. 141, pp. 56–67, 2022.
- [4] Hemlata Tak, Madhu Kamble, Jose Patino, Massimiliano Todisco, and Nicholas Evans, “Rawboost: A raw data boosting and augmentation method applied to automatic speaker verification anti-spoofing,” in *Proc. ICASSP*, 2022, pp. 6382–6386.
- [5] Xin Wang and Junichi Yamagishi, “Investigating self-supervised front ends for speech spoofing countermeasures,” in *Proc. Odyssey*, 2022, pp. 100–106.
- [6] Zihan Pan, Tianchi Liu, Hardik B. Sailor, and Qiongqiong Wang, “Attentive merging of hidden embeddings from pre-trained speech model for anti-spoofing detection,” in *Proc. Interspeech*, 2024.
- [7] Yuankun Xie, Haonan Cheng, Yutian Wang, and Long Ye, “Domain generalization via aggregation and separation for audio deepfake detection,” *IEEE Transactions on Information Forensics and Security*, vol. 19, pp. 344–358, 2023.
- [8] You Zhang, Fei Jiang, and Zhiyao Duan, “One-class learning towards synthetic voice spoofing detection,” *IEEE Signal Processing Letters*, vol. 28, pp. 937–941, 2021.
- [9] Andrew Ustinov, Matey Yordanov, Andrei Kuchma, and Mikhail Bychkov, “Cross-technology generalization in synthesized speech detection: Evaluating ast models with modern voice generators,” *arXiv preprint arXiv:2503.22503*, 2025.
- [10] Jindong Wang, Cuiling Lan, Chang Liu, et al., “Generalizing to unseen domains: A survey on domain generalization,” *IEEE transactions on knowledge and data engineering*, vol. 35, no. 8, pp. 8052–8072, 2022.
- [11] Yaroslav Ganin, Evgeniya Ustinova, Hana Ajakan, et al., “Domain-adversarial training of neural networks,” *Journal of machine learning research*, vol. 17, no. 59, pp. 1–35, 2016.
- [12] Xin Wang, Junichi Yamagishi, Massimiliano Todisco, et al., “Asvspoof 2019: A large-scale public database of synthesized, converted and replayed speech,” *Computer Speech & Language*, vol. 64, pp. 101114, 2020.
- [13] Junichi Yamagishi, Xin Wang, Massimiliano Todisco, et al., “Asvspoof 2021: accelerating progress in spoofed and deepfake speech detection,” *arXiv preprint arXiv:2109.00537*, 2021.
- [14] Xin Wang, Héctor Delgado, Hemlata Tak, et al., “Asvspoof 5: Crowdsourced speech data, deepfakes, and adversarial attacks at scale,” *arXiv preprint arXiv:2408.08739*, 2024.
- [15] Naftali Tishby, Fernando C Pereira, and William Bialek, “The information bottleneck method,” *arXiv preprint physics/0004057*, 2000.
- [16] Alexander A. Alemi, Ian Fischer, Joshua V. Dillon, and Kevin Murphy, “Deep variational information bottleneck,” in *Proc. ICLR*, 2017.
- [17] Yujie Chen, Jiangyan Yi, Jun Xue, et al., “Rawbmamba: End-to-end bidirectional state space model for audio deepfake detection,” in *Proc. Interspeech*, 2024.
- [18] Xin Wang and Junichi Yamagishi, “Spoofed training data for speech spoofing countermeasure can be efficiently created using neural vocoders,” in *Proc. ICASSP*, 2023, pp. 1–5.
- [19] Diederik P. Kingma and Jimmy Ba, “Adam: A method for stochastic optimization,” in *Proc. ICLR*, 2015.
- [20] Ashish Vaswani, Noam Shazeer, Niki Parmar, et al., “Attention is all you need,” in *Proc. NIPS*, 2017, vol. 30, pp. 5998–6008.
- [21] David Snyder, Guoguo Chen, and Daniel Povey, “Musan: A music, speech, and noise corpus,” *arXiv preprint arXiv:1510.08484*, 2015.
- [22] Tom Ko, Vijayaditya Peddinti, Daniel Povey, Michael L. Seltzer, and Sanjeev Khudanpur, “A study on data augmentation of reverberant speech for robust speech recognition,” in *Proc. ICASSP*, 2017, pp. 5220–5224.
- [23] Hemlata Tak, Massimiliano Todisco, Xin Wang, Jee-weon Jung, Junichi Yamagishi, and Nicholas W. D. Evans, “Automatic speaker verification spoofing and deepfake detection using wav2vec 2.0 and data augmentation,” in *Proc. Odyssey*, 2022, pp. 112–119.
- [24] Jingze Lu, Yuxiang Zhang, Wenchao Wang, Zengqiang Shang, and Pengyuan Zhang, “One-class knowledge distillation for spoofing speech detection,” in *Proc. ICASSP*, 2024, pp. 11251–11255.
- [25] Zhiyong Wang, Ruibo Fu, Zhengqi Wen, et al., “Mixture of experts fusion for fake audio detection using frozen wav2vec 2.0,” in *Proc. ICASSP*, 2025, pp. 1–5.
- [26] Qishan Zhang, Shuangbing Wen, and Tao Hu, “Audio deepfake detection with self-supervised XLS-R and SLS classifier,” in *Proc. ACM Multimedia*, 2024, pp. 6765–6773.
- [27] Wen Huang, Yanmei Gu, Zhiming Wang, Huijia Zhu, and Yanmin Qian, “Generalizable audio deepfake detection via latent space refinement and augmentation,” in *Proc. ICASSP*, 2025, pp. 1–5.
- [28] Yang Xiao and Rohan Kumar Das, “Xlsr-mamba: A dual-column bidirectional state space model for spoofing attack detection,” *IEEE Signal Processing Letters*, 2025.
- [29] Tianchi Liu, Duc-Tuan Truong, Rohan Kumar Das, Kong Aik Lee, and Haizhou Li, “Nes2net: A lightweight nested architecture for foundation model driven speech anti-spoofing,” *arXiv preprint arXiv:2504.05657*, 2025.